Physicochem. Probl. Miner. Process. 48(2), 2012, 513−531

www.minproc.pwr.wroc.pl/journal/

Physicochemical Problems of Mineral Processing

ISSN 1643-1049 (print)
ISSN 2084-4735 (online)

Received April 13, 2011; reviewed; accepted May 10 , 2012

EFFECTS OF DIFFERENT MESH SCHEMES AND TURBULENCE MODELS IN CFD MODELLING OF STIRRED TANKS

Mohsen KARIMI, Guven AKDOGAN, Steven M. BRADSHAW

Department of Process Engineering, Stellenbosch University, Private Bag X1, Matieland 7602, Stellenbosch, South Africa. Tel: +27 21 808 3860, Fax: +27 21 808 2059; Email: karimi@sun.ac.za

Abstract. This paper focuses on the effects of grid schemes and turbulence models on the CFD modelling of stirred tanks. The economical grid was determined by examining the dimensionless wall distance and the skewness of elements. The grid independency study ensured that the independency of numerical predictions. Also, three categories of turbulence models were compared for prediction of flow pattern. The grid sensitivity study highlighted that the quality of control volumes in the bulk and near the wall regions are significant for obtaining the consistent solutions. It was also found that for the prediction of velocity components and the turbulent quantity the RANS based models are more efficient.

keywords: stirred tank, computational fluid dynamics, turbulence models, grid sensitivity

1. Introduction

Mechanically stirred vessels are broadly used in a wide range of unit operations such as flotation cells in mineral processing plants, blending of liquids and crystallization in chemical engineering reactors. Owing to their extensive range of use, a reliable method of simulating the hydrodynamics of flow instead of correlating the overall performance to the operational and geometrical conditions would be beneficial for the industries.

Computational Fluid Dynamics (CFD) provides a numerical method in which thorough information on the hydrodynamics of fluid flow can be extracted. The flow pattern is then used to understand the details of the process itself. Thus, it would be expected that an accurate CFD simulation of the fluid flow leads to improved understanding of the mixing sub-processes occurring in mechanically stirred vessels.

Since the unsteady nature of turbulent flow inside stirred tanks is affected by many parameters such as the geometry of rotational system, the local vortices, the gas dispersion and so on, an accurate simulation of the flow pattern is rather complex. To tackle this intricate problem one may investigate the factors such as the grid resolution, the discretization scheme, the impeller rotation modelling method, and the turbulence models. At the same time, the enhancement of CFD packages is an on-going progress, and each new version of solvers is equipped with more features aimed

http://dx.doi.org/10.5277/ppmp120216

at accurately capturing more details of the fluid flow behaviour. As a consequence, a computationally efficient and accurate CFD model for a stirred tank must be updated to assess the effects of new options encompassed in recent CFD solvers. In the insight of previous works that considered different aspects of CFD modelling of a stirred tank, this research is scoped to update and optimize the CFD methodology for stirred tanks as realistic as possible, while it should be computationally inexpensive.

The potential of CFD for modelling of unbaffled stirred tanks has been reported in several papers. The applicability of numerical modelling was demonstrated by comparison of the simulated results with the laser-Doppler velocimeter data (Armenante et al., 1997; Dong et al., 1994a, b). In these early papers, the standard k-ε and the Algebraic Stress Model (ASM) were used as turbulence models and the rotation of impeller was modelled by either adapting the LDV measurements or by the Multiple Reference Frames (MRF) method.

Oshinowo et al. (2000) showed that MRF is an efficient choice for the modelling of impellers in the baffled stirred tanks. The sensitivity of the solution to the different grids was also investigated. They compared the predicted tangential velocities with the three turbulence models including the standard k-ε, the RNG k-ε and RSM. They concluded that the steady-state modelling with the MRF is a valuable tool in the analysis and design of stirred tanks when the single phase turbulent flow occurs.

Bakker (Bakker and Oshinowo, 2004; Bakker et al., 2000) investigated whether the Large Eddy Simulation (LES) can predict the large-scale chaotic structures in stirred tanks. A single radial pumping impeller and a single axial pumping pitched blade turbine were simulated. The results showed that both impeller configurations had qualitatively good agreement with the experimental data (Myers et al., 1997).

Another approach for modelling of impellers, the Sliding Mesh method (SM), was compared with the MRF by Lane et al. (2000). The computational time, accuracy of mean velocities and the turbulence parameters were the main variables of comparison. A half slice model of a 294 mm diameter baffled stirred tank was discretized by 48, 39 and 60 cells in the axial, radial and azimuthal directions. An important finding was that the MRF method was more computationally efficient than the SM. They also found that both methods had similar results for the prediction of the velocities. For turbulence characterizations, the MRF provided an improvement in the predictions.

Yoon et al. (2001) modelled the motion of impellers using Particle Image Velocimetry (PIV) data as boundary conditions around the impeller. A 3D grid of 51,840 cells for 60° sector of a 145 mm diameter cell was used to compute the flow. They provide a method to describe the impeller-induced flow in the stirred tank.

Influences of different impeller modelling methods, discretization schemes, and turbulence models on the CFD modelling of stirred tanks were investigated by Aubin et al. (2004). The mean axial and radial flow patterns were slightly affected by the choice of SM or MRF for modelling of the impeller. The higher order of discretization schemes were recommended for the simulation of turbulent flow inside the stirred tank. Applying the Reynolds Stress Model (RSM) as the turbulence model led to a

diverged solution. The Standard and the Renormalization-group k-ε models did not show significant differences in predicting the mean radial and axial velocity fields. The authors suggested that correct prediction of the single phase flow quantities is necessary for an accurate multiphase modelling of stirred tanks.

Deglon and Meyer (2006) used the MRF for modelling of the impeller rotation in conjunction with the standard k-ε turbulence model for studying the turbulence effects. The flow pattern in a half of a cylindrical tank agitated with a standard six-blade Rushton turbine was simulated over four different grids using the QUICK discretization scheme. A range of impeller speeds corresponding to the laminar and turbulent flow regimes were tested. They showed that although the flow field can be predicted with a coarse mesh, an accurate prediction of turbulence in stirred vessels is computationally intensive and needs both fine grid resolution and a high-order discretization method.

One of the recent work addressing numerical issues in the CFD simulation of the fluid flow in stirred tanks was performed by Coronoe (2010). This work aimed at verifying the effect of numerical issues on the RANS-based predictions of the single phase flow in stirred tanks. The effects of grid sizes and discretization schemes were considered for modelling of the mean velocity, the turbulent dissipation, and the homogenization with the standard k-ε turbulence model and the MRF method. This work revealed that the effect of numerical uncertainties may be minimized with sufficiently fine grid resolution. They argued that due to the limitation of the turbulence model the detailed explanation of turbulence quantities cannot be achieved. They also mentioned that the effects of the numerical inaccuracies would be more important in the multiphase modelling of stirred tanks.

Reviewing the previous literature revealed that the standard k-ε is a computationally affordable turbulence model and it is generally accepted for the modelling of stirred tanks. The Multiple Reference Frames (MRF) yields better results than the Sliding Mesh method to model the impeller motion in terms of both computational time and agreement with the experimental data. Although the previous works shed some light on how to deal with the common aspects of the numerical issues on the CFD modelling of stirred tanks, CFD solver developments led to the question of whether the available methodology of numerical simulation of the stirred vessel is still reliable or it should be updated. Thus, this paper is intended to fill this gap. To accomplish this goal, the optimized mesh was selected through different criteria including the value of y+ on the problematic regions near the walls to capture the small eddies, skewness of elements, and the grid independence study. Then, turbulence models were categorized into three different groups. The performance of each category was compared with the experimental data.

2. Methodology

The Reynolds averaged continuity and the Reynolds averaged Navier-Stokes equations (RANS) have been resolved in this work to model the highly turbulent flow inside the agitated vessel. They can be written as follow:

$$\frac{\partial \rho}{\partial t} + \rho \frac{\partial \langle u_i \rangle}{\partial x_i} = 0 , \tag{1}$$

$$\frac{\partial \left(\rho \langle u_i \rangle\right)}{\partial t} + \frac{\partial \left(\langle u_i \rangle \langle u_j \rangle\right)}{\partial x_j} = \frac{\partial \langle p \rangle}{\partial x_i} + \frac{\partial}{\partial x_j}\left(\mu \frac{\partial \langle u_i \rangle}{\partial x_j}\right) + \frac{\partial}{\partial x_j}\left(\tau_{ij}^{\mathrm{Re}}\right) + \rho g_i , \tag{2}$$

where u is the velocity component, ρ is the liquid density, p is the pressure, μ is the fluid viscosity, and g is the gravitational acceleration. The term τ_{ij}^{Re} denotes the Reynolds stress and signifies the effects of turbulent velocity fluctuations on the mean flow. To close Eqs. (1) and (2) the Reynolds stress must be modelled. There are different turbulence models to achieve closure for the above partial differential equations. In the following sections the fundamentals of these models are briefly explained and referenced.

2.1. RANS based turbulence mode

The RANS-based turbulence models are recommended (ANSYS Inc, 2009) to reduce the required computational effort and resource. They are divided into the four different categories including: one-equation model, two-equation models, three-equation models, and Reynolds Stress Model (RSM). Except the latter, the other RANS-based turbulence models apply the Boussinesq hypothesis (Hinze, 1975) that relates the Reynolds stresses to the mean velocity gradients:

$$\tau_{ij}^{\mathrm{Re}} = u_t \left(\frac{\partial u_i}{\partial x_j} + \frac{\partial u_j}{\partial x_j}\right) - \frac{2}{3}\left(\rho k + \mu_t \frac{\partial u_k}{\partial x_k}\right)\delta_{ij} . \tag{3}$$

In this equation μ_t is the turbulent viscosity, k is the turbulent kinetic energy and δ_{ij} is the Kronecker delta. The Boussinesq theory assumes the turbulent viscosity is an isotropic scalar.

The RANS-based turbulence models have been divided according to the number of additional transport equations essential to resolve the flow field.

2.1.1. One-equation model

The Spalart-Allmaras is a relatively simple one-equation model that solves one transport equation for the turbulent kinematic viscosity. The details of equations of this model are explained by Spalart and Allmaras (1992).

2.1.2. Two-equation models

This group of turbulence models has become the standard approach for industrial applications and is of particular interest for engineering problems where turbulence effects are significant such as stirred vessels. As the definition states, to capture the

turbulence effects, two extra transport equations must be solved for this type of turbulence model. Models such as the k- ε and its variants and the k-ω model and its variant fall into this class. From two additional transport equations, one of the variables is turbulent kinetic energy, *k*. The second one depends on what type of two-equation turbulence models is used. The second transported variable can be thought of as the determination factor of turbulence. The common options for the two-equation models are the turbulent dissipation, ε, or the specific dissipation, ω.

- Standard k-ε model

The advantages of using the Standard k-ε model such as robustness and reasonable accuracy account for the numerous applications of this model in the simulation of stirred tanks. The standard k-ε model is a semi-empirical model that solves the turbulent kinetic energy (k) and its turbulent dissipation (ε) for fully turbulent flow. The details of the transport equations were explained by Launder and Spalding (1972).

- RNG k-ε model

The RNG k-ε model is derived from the standard k-ε model carrying out a mathematical technique called "renormalization group" (RNG). In this turbulence model some refinements for accurate results have been outlined. Adding an extra term in the "ε" equation improves the accuracy for rapidly strained flows. Besides, the effects of swirl on the turbulence are included in the RNG k-ε model, enhancing the precision for swirling flow. Orszag et al. (1993) have documented a complete application of the RNG concept for turbulence modelling.

- Realizable k-ε model

This turbulence model is a relatively new approach to resolve the Reynolds stresses (Shih et al., 1995). Its differences from the standard k-ε model are twofold: a new formulation for the turbulent viscosity and a vorticity-based new transport equation for the turbulent dissipation, ε. These modifications are reported to provide superior performance for swirling flow.

- Standard k-ω model

The standard k-ω model used in this paper is based on the Wilcox k-ω model (Wilcox, 1998). Wilcox has derived this empirical turbulence model based on the transport equations for turbulence kinetic energy (k) and the specific turbulent dissipation (ω).

- Shear-Stress Transport (SST) k-ω model

Blending the robust formulation of the k-ω model in the inner parts of boundary layer with the applicability of the k-ω model in the bulk flow is the backbone of this model. The SST k-ω turbulence model was developed by Menter (1994).

- Transition SST model

The transition SST model is another derivative of the k-ω model taking advantage of two more transport equations, one for intermittency and one for the transition onset criteria.

2.1.3. Three-equation model

- k-kl-ω transition model

Since the k-kl-ω model has three transport equations for the turbulent kinetic energy, the laminar kinetic energy, and the inverse turbulent time scale (ω), it is considered as a three-equation model. This model benefits from predicting the boundary layer development and the calculating transition onset. Using this model one can effectively address the evolution from laminar flow to turbulence in the boundary layer.

2.2. Large Eddy Simulation (LES)

The entire concept of the Large Eddy Simulation (LES) model is based on eddies that are the main characteristics of the turbulent flow. In this model, the motion of large eddies is resolved directly, while the small eddies are implicitly modelled using a sub-grid scale model. Thus, a filtering operation should be conducted to separate the velocity field into two resolved parts; large eddies and a sub-grid part. Filtering the time-dependent Navier-Stokes equations results in a set of the solved part (large scale) and the residuals (small scale). The filtered equations are expressed as:

$$\frac{\partial \rho}{\partial t} + \rho \frac{\partial \overline{u_i}}{\partial x_i} = 0\,, \tag{4}$$

$$\frac{\partial \overline{u_i}}{\partial t} + \frac{\partial \left(\overline{u_i}\,\overline{u_j}\right)}{\partial x_j} = -\frac{1}{\rho}\frac{\partial \overline{p}}{\partial x_t} + \frac{\partial}{\partial x_j}\left(\mu \frac{\partial \overline{u_i}}{\partial x_j}\right) - \frac{\partial \tau_{ij}^{sgs}}{\partial x_j} + g_i\,, \tag{5}$$

τ_{ij}^{sgs} is the stress tensor composed of all the information about small scales. It can be related to the eddy viscosity by the following equation:

$$\tau_{ij}^{sgs} = -\mu_t\left(\frac{\partial \overline{u_i}}{\partial x_j} + \frac{\partial \overline{u_j}}{\partial x_i}\right). \tag{6}$$

In this research, solving the eddy viscosity, μ_t, has been conducted by three different methods: Smagorinsky-Lilly (Smagorinsky, 1963), WALE model (Nicoud and Ducros, 1999), and dynamic kinetic energy (Kim and Menon, 1997).

2.3. Detached Eddy Simulation

The DES model is a hybrid turbulence model that applies the RANS model to solve the flow near the wall, and other regions far from the walls are computed by the LES approach. In the modelling of stirred tanks in this study three combinations of RANS models with the LES have been considered including the Spalart-Allmaras, realizable k-ε and the SST k-ω (Shur et al., 1999). It should be noted here that computational

cost of using DES model is greater than the RANS computational cost, but less than the LES.

3. Numerical approach

The 3D unsteady flow of water inside a 293 mm diameter unbaffled tank agitated by a six-blade impeller with 73 mm clearance (Fig. 1) was simulated using CFD package ANSYS FLUENT 12.1. Since the finite volume method is implemented in this solver, the computational domain, adopted from (Armenante et al., 1997), was discretized into different cells. To conduct the MRF method for modelling of impeller motion, recommended by Lane et al. (2000) and Deglon and Meyer (2006), the entire vessel was divided into the bulk flow region and the rotational zone. In this way, governing equations are solved in a rotating reference frame to handle the impeller rotation, while in the rest of the vessel the flow is calculated by solving the RANS equations in a stationary reference frame. The SIMPLE algorithm coupled the continuity and momentum equations to derive the pressure field inside the tank, and the momentum discretization was computed by a second-order upwind method. It should be mentioned that to perform the LES and DES turbulence models the discretization scheme was altered to the bounded central differencing method. In this study, the impeller speed was 450 rpm. A 45° sector of vessel was simulated using periodic boundary conditions.

Different time steps corresponding to 5, 10, 12 and 15 degrees of rotational angle of the impeller have been simulated. Each simulation was initialized with the standard k-ε turbulence model for 10 revolutions of the impeller. All the simulations were performed on an Intel Corei7 CPU 1.6 GHz workstation in this study.

One of the main issues that have been considered in this article is how sensitive the CFD results are to the various mesh schemes. The grid density should be dense enough to embody all the underlying flow features. To explain this effect, different grids have been built up. In each case, different numbers of elements in the two separate regions, the bulk flow and the rotational zone, have been distinguished. The details of each structured hexagonal mesh are described in Table 1. The number of elements in the three directions of cylindrical coordinate system is shown in Table 1.

In order to capture the time-dependent fluctuations of turbulence inside the boundary layer, y+ value was taken into account. These parameters are defined as the dimensionless distance from the wall to the first grid point. The value of y+ is computed for the boundary cells on the specified wall zones. Then, those cells with the y+ values within a specified range will be marked for refinement during the solution process. The y+ can be computed by the following equation:

$$y+ = \frac{u^* y}{\nu}, \tag{7}$$

where u^*, the friction velocity can be defined by Eq. (8), y is the distance to the wall and ν is the kinematic viscosity:

$$u^* = \sqrt{\frac{\tau_w}{\rho}}, \tag{7}$$

where τ_w is the wall shear stress and ρ is the fluid density at the wall.

Skewness has also been used in this study to investigate the quality of each control volume. As is shown in Table 1, even the maximum skewness is in the excellent range of commonly used for the mesh quality (ANSYS Inc, 2009).

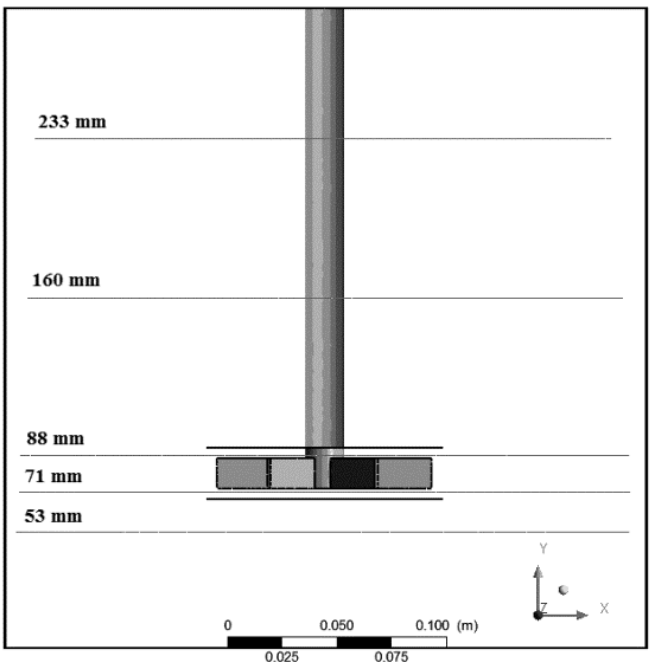

Fig. 1. Schematic of the whole vessel adapted from Armenante et al. (1997)

Table 1. Properties of the mesh schemes used in this article

Case#	Bulk flow			Rotational zone			No. Cells		Skewness		
	ρ	φ	z	ρ	φ	z	Original	Adapted	Min	Max	Ave
C1	31	20	65	11	20	5	40,300	59,375	0.0125	0.1086	0.0242
C2	40	24	78	14	24	6	74,880	110,762	0.0104	0.1429	0.0190
C3	48	29	94	17	29	8	130,848	176,306	0.0050	0.0990	0.0211
C4	58	35	113	20	35	10	229,390	296,478	0.0041	0.1077	0.0168
C5	70	42	126	24	42	12	370,440	472,129	0.0034	0.1260	0.0210
C6	84	50	139	29	50	14	583,800	704,818	0.0029	0.1436	0.0208
C7	92	60	154	35	60	17	850,080	1,024,317	0.0015	0.1606	0.0309

* the numbers in the ρ,φ, and z columns represent the number of elements in each direction of cylindrical coordinate system

4. Results and discussion

4.1. Grid study

As the grid determines the control volume on which all governing equations for the stirred tank are resolved, the numbers of cells directly affect the solution accuracy and the required CPU time. One of the main aspects of this study is to examine the influences of different cell numbers on the prediction of flow behaviour. Therefore, finding the optimized number of cells wherein almost all the local turbulent events are captured, yet the computational time is affordable, is one of the focal points of this work. Meanwhile, the quality of an efficient mesh should be good enough so that the solution is not affected by the bad-quality elements. Owing to the facts mentioned above, the skewness and values of the y+ were utilised for surveying the mesh quality in the bulk flow and the viscous layer near the wall.

4.1.1. Systematic study of y+

In the turbulent flow in a stirred tank, the mean flow is strongly affected by the turbulence. The numerical results for this type of flow depend on the mesh size. It would be expected that a sufficiently fine mesh for the regions where the mean flow is influenced by the existence of the rapid changes and the shear layers with large strain rates can resolve the flow field pattern. Values of y+ can be an indicator for checking the near-wall mesh quality. Two different wall functions namely, the standard wall function, which is the most widely used in the industrial flows and the enhanced wall treatment, appropriate for the fine mesh schemes, were applied for capturing the near-wall flow features. It is recommended (ANSYS Inc, 2009) that for using the standard wall function, the value of y+ in the first cell should be within the logarithmic law layer, whereas the enhanced wall treatment requires y+ as low as possible ($y+<5$). Testing the value of y+ at all bounding walls showed that the most problematic area is the blade region. Figure 1 shows the value of y+ on the centre line of the blade for different number of meshes. It is clearly shown that the highest value in all cases is at the tip and close to the impeller-shaft junction point.

To reduce the value of y+ on the blade, the solution-adaptive mesh refinement feature of ANSYS FLUENT was used. In this way, additional cells can be added where they are needed, which is in this case on the tip and close to the shaft. The main advantage of this method is that one can locally increase the number of cells based on the solution and analyse the impacts of supplementary cells on the results without regenerating of the mesh. Different refinement methods have been applied on the problematic areas. After comparing different adaptation methods, results of the best refinement that decreases the value of y+ more than other approaches are depicted in Fig. 2. The number of cells after refinement is reported in Table 1.

In order to assess how much the extra cells change the maximum y+ value on the blade, the simulations were repeated after the refinement. All other simulation parameters were kept constant. The values of y+ on the centre line of the blade are

displayed in Fig. 2. Except for the first case, maximum y+ value on the blade in all the other cases is significantly decreased.

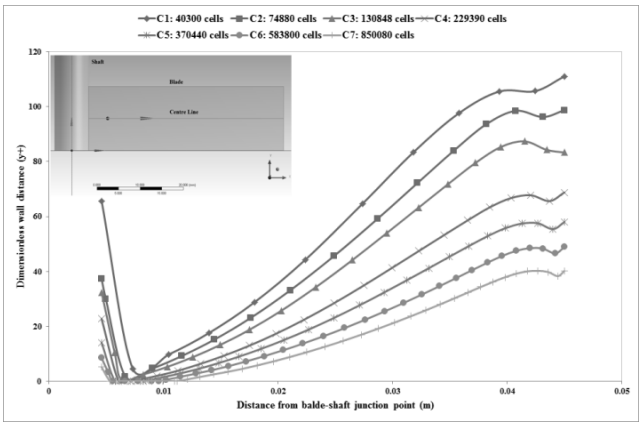

Fig. 2. Value of y+ on the centre line of blade for seven different cases before refinement. C1 to C7 represent the number of cells before refinement for case1 to case7 described in Table 1

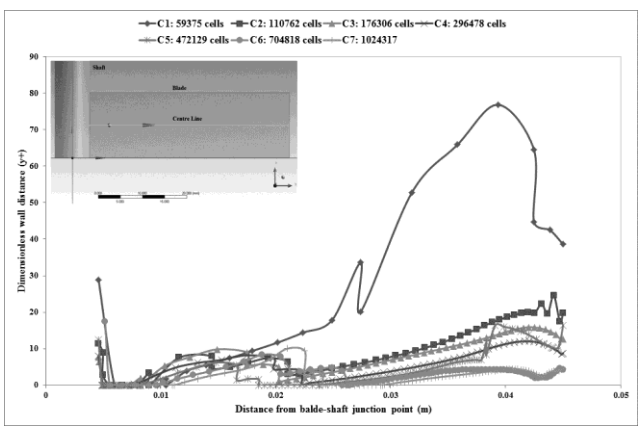

Fig. 3. Value of y+ on the centre line of blade for seven different cases after refinement. C1 to C7 represent the number of cells after refinement for case1 to case7 described in Table 1

It can also be seen from Fig. 2 that for case 6 and case 7 the values of y+ are coincident. Thus, adding more cells did not lead to improvement in the value of y+. To elaborate more on this behaviour the maximum y+ on the centre line for the seven different cases is plotted with respect to computational time in Fig. 3. The number of cells in Fig. 3 is adopted after the refinement. Although the reduction rate of y+ maximum on the blade for the first three cases (i.e. C1 with 59375 cell, C2 with 110762 cells and C3 with 176306 cells) is too high, it is clearly demonstrated that beyond certain number of cells the maximum value of y+ does not differ significantly. Since the computational time and number of cells are following a linear correlation,

using high number of cells results in increasing the required CPU time without reducing the maximum y+. Also, an extreme case with 2 million cells was investigated and the effect on the y+ was found to be insignificant while the computational time was around 48 hours. The systematic study of y+ suggests that successful computation of turbulent flow close to the walls of the stirred tank can be achieved by a grid density between 500,000 to 700,000 cells. Figure 4 illustrates the contour plot of y+ for the case with 704, 818 cells. The final refined surface mesh on the blade is also shown in this figure.

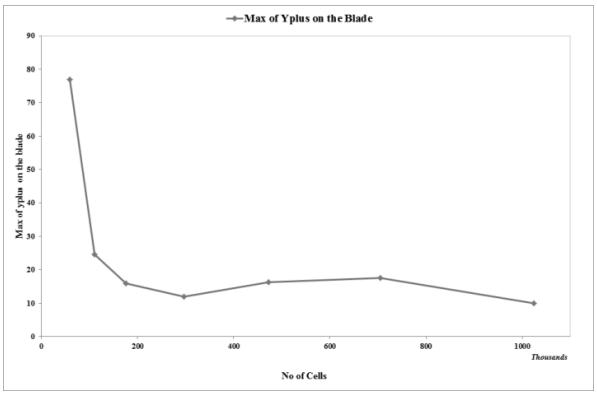

Fig. 4. Maximum y+ value on the centre line of the blade for seven different cases

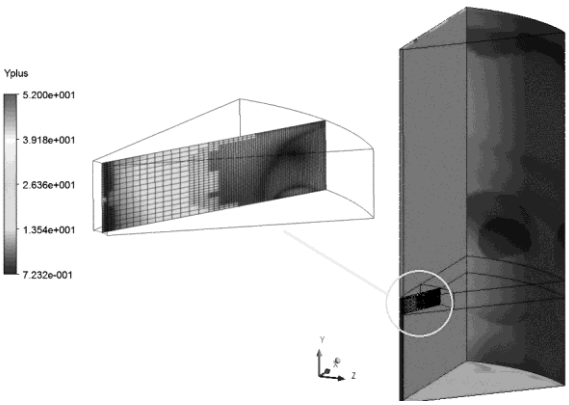

Fig. 5. Contour plot of y+ value for 45° sector and blade

4.1.2. Grid independence study

Any small fluctuations of velocity and other features of the flow within the tank should be captured by an efficient mesh scheme. However, a very fine mesh refinement leads to increased computational time. Thus, a grid independence study has been performed to find optimize number of cells for which the solution is independent.

To achieve this aim, four points on five planes in different parts of the vessel were defined (Fig. 5). As shown in Fig. 5, the planes covered all the hydrodynamically significant zones of the tank such as lower bottom of the vessel, top and bottom of the impeller and two planes for the upper parts of the vessel. The points are also situated in the locations where the data close to the impeller, shaft, middle of vessel and close to the wall can be derived. After running the simulations for seven cases (Table 1) the values of the velocity components (tangential, radial and axial) and the turbulent kinetic energy were collected for all the nominated points, shown in Fig. 5, to quantify how much each of these components vary over the wide-ranging numbers of cells. Because of space constraints, only the results of tangential velocity and turbulent kinetic energy in the middle of each plane, depicted by the balls in Fig. 5, are shown here.

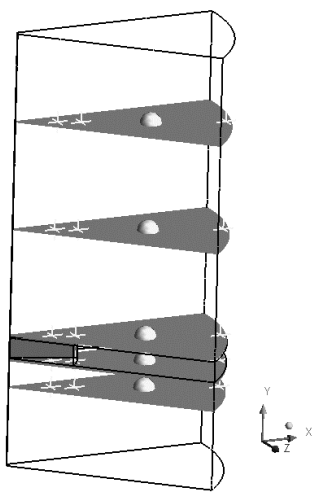

Fig. 6. Locations of points and planes for the grid sensitivity test (the whole vessel and 45º sector)

Figures 7 and 8 show the variations of tangential velocity and turbulent kinetic energy at the selected points for the different numbers of cells. It is clearly demonstrated here that there exists a specific grid size beyond which both the velocity components and the turbulent quantities show little variation. It is seen in Fig. 6 a-c and e that variations of tangential velocity are negligible after the number of 472,000 elements (case 5), although for the plane 160 mm from the bottom of vessel (Fig. 6d) this observation is seen for 704,000 cells.

From Fig. 8 it can be seen that increasing the number of cells to 1000,000 means that one can detect only very small eddies inside the computational domain and the mean quantity of turbulent kinetic energy does not change significantly. It must be noted that the simulated data (the velocity components and the turbulent kinetic energy) for the other points were also checked but results, for the sake of brevity, are not included in the present paper.

Therefore, in order to have the precise and computationally economical solution the y+ systematic study in combination with the grid independence study should be conducted. The results of these two examinations show that the adopted grid system applied in the case 6 (Table 1) can computes the flow close to the boundary layers, while at same time the general phenomenon of the bulk flow can be predicted thoroughly. As a result the methodology used for case 6 (Table 1) was chosen to investigate the effects of different turbulence models in the simulation of flow field within the stirred vessel.

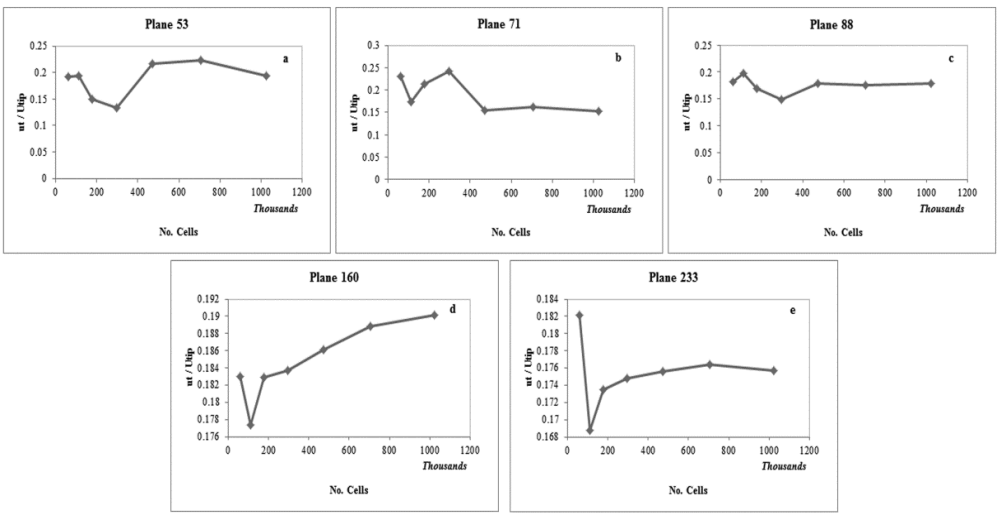

Fig. 7. Tangential velocities for the mid-points in five different palnes, shown in Fig. 6, for different grids

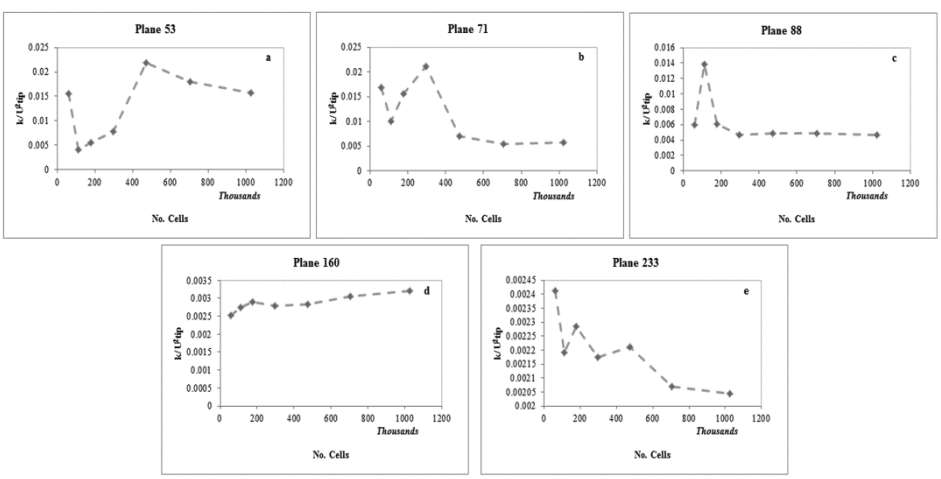

Fig. 8. Turbulent kinetic energy for the mid-points in five planes for different grids

4.2. Turbulence models study

There is no generally accepted turbulence model that can be applied in all types of engineering flow simulation problems. Therefore, a comparison of different turbulence models for prediction of flow inside the stirred tank is another aim of this work. To attain this objective all the turbulence models available in ANSYS FLUENT 12.1 were categorized into various groups based on their methodology of calculation of the term τ_{ij}^{Re} in Eq. (2). Also, the experimental data, adopted from Armenante et al. (1997), were used to compare the performance of each turbulence model for estimation of the velocity components and the turbulence quantity. The selected results for each group are discussed in the following sections.

4.2.1. Validation of RANS turbulence models

As discussed in the methodology section, this type of turbulence model implements the Boussinesq assumption that relates Reynolds stresses to the mean velocity gradient. Because this group of turbulence models solves the averaged flow quantities they are computationally preferable.

For the validation of each model, the velocity components (tangential, radial and axial) as well as the turbulent kinetic energy were compared with the experimental data over five different planes (Fig. 5). It should be mentioned among all the RANS models, using the Reynolds Stress Model (RSM) led to diverged solutions. Attempt to remedy this by decreasing the under-relaxation factors, initializing with the other turbulence models, gradually increasing the angular velocity and varying the time step were unable to achieve a converged solution.

Figure 9 shows the tangential velocity profile predicted by the RANS models together with the experimental data. It is clear that the choice of turbulence models plays an important role in the simulation of the flow inside the stirred tank. Among the models with the scalar assumption of turbulent viscosity, the k-ε RNG and the Transition-SST turbulence models provided a better fit to the experimental data. Although the Transition-SST predicted the maximum of velocity closer to the experimental data, the general trend of the k-ε RNG data for the rest of the vessel compared well with the experimental data.

Comparing the axial and the radial velocity profiles on the other planes showed that the performances of the above mentioned models, the k-ε RNG and the Transition-SST, were better than other RANS models. Transition SST for predicting the axial velocity was the efficient option, while the radial velocity profiles predicted with the k-ε RNG were more accurate. In the regions with high turbulence, i.e. the impeller discharge zone and the bottom of the vessel, the prediction of turbulent kinetic energy with the three-equation turbulence model, k-kl-ω, was significantly improved and the transition SST worked better for the top part the vessel where the flow was not influenced too much due to the rotation of the impeller.

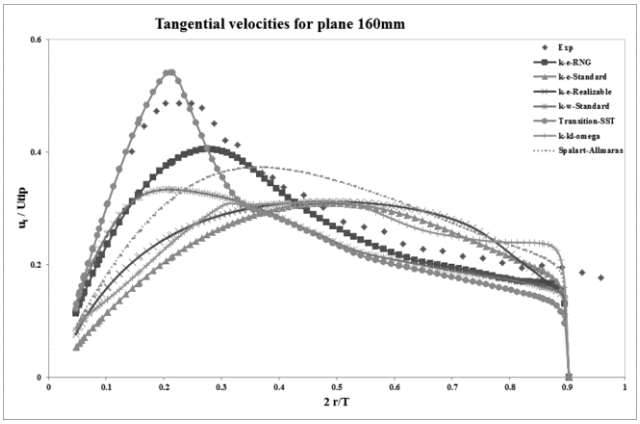

Fig. 9. RANS predictions of tangential velocity compared with experimental data for plane 160

4.2.2. Validation of Large Eddy Simulation (LES)

The tangential velocity profile on plane 160 predicted by the LES is compared with the experimental data in Fig. 10. In order to assess the performance of LES model for calculation of eddy viscosity, μ_t (Eq. (6)), three approaches have been applied. As is demonstrated in Fig. 10, these three subgrid-scale models have very good agreement with the LDV results. The maximum of velocity at the tip is slightly over-predicted by the Smagorinsky-Lilly and the WALE approaches, though it is captured by the "kinetic energy transport" method. This conclusion is also valid for the other planes.

To predict the axial velocity the WALE model provides results comparable to the "kinetic energy" alternative and both of them have captured the trends of the axial velocity measurements.

The radial velocity profile predictions with these three subgrid-scale models fit the measurements fairly well, and none of the subgrid-scale models has any merit in terms of having closer agreement with the experimental data. As the fluctuation range of this velocity component is very narrow, having exact fit with the experimental data is computationally very expensive. It is interesting to note that among the three subgrid-scale models one may select the "kinetic energy" method to justify the term optimized methodology, i.e. having both adequate agreement with experimental data and reasonable computational cost.

4.2.3. Validation of Detached Eddy Simulation (DES)

The Detached Eddy Simulation model draws advantages from the RANS models to predict the flow behaviour close to the wall and the LES in the rest of the stirred tank. Three RANS models involving the Spalart-Allmaras, realizable k-ε, and SST k-ω in combination with the LES have been tested to simulate the flow pattern inside the vessel. As a case to illustrate the performance comparison, Fig. 11 shows the tangential velocity profile on the plane 160 mm from the bottom of the tank. There is

not much difference among these three turbulence models, nevertheless the maximum velocity predicted by the combination of LES/realizable k–ε was in better agreement with the experimental data.

Generally, for prediction of the radial and axial velocity components, the above-mentioned combination fits the LDV data fairly well. Comparison of the simulated turbulent kinetic energy with the experimental data showed that the Detached Eddy Simulation method was not suitable to predict the measured data. Its under-predictions of turbulent kinetic energy are problematic for its use as a turbulence model for a stirred tank.

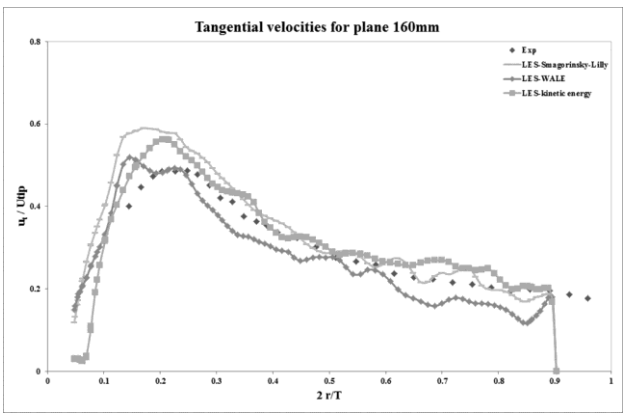

Fig. 10. LES predicitons of tangential velocity compared with experimental data for plane 160

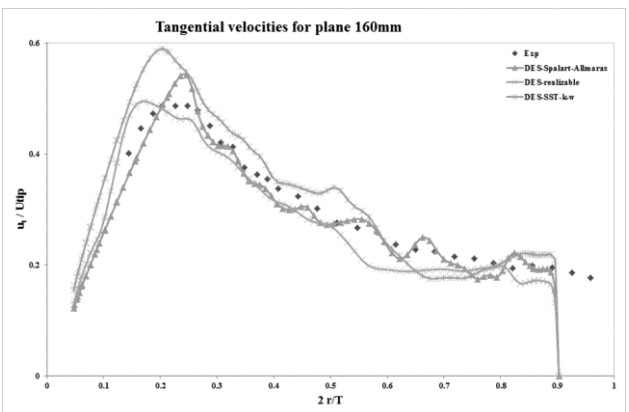

Fig. 11. DES predictions of tangential velocity compared with experimental data for plane 160

4.2.4. Comparison of different turbulence models

Validation of each turbulence model in the previous sections showed that the choice of turbulence model was an inseparable part in the simulation of stirred tanks.

The models in which the Boussinesq hypothesis is applied found to be more adequate for the stirred tank modelling. The Spalart-Allmaras, k-ε family, k-ω family are computationally efficient and inexpensive. The Spalart-Allmaras was found to be the least expensive model in this paper. However, LES, based on the modelling of the large-scale eddies, needed longer CPU times to obtain a stable solution compared to the RANS model. The advantage of using the RANS/LES hybrid model might be that the computational cost falls between LES and RANS models.

All the three groups of turbulence models have also been compared with experimental data. To accomplish this comparison, the optimized model was selected in such a way that two criteria of having short computational time and acceptable agreement with the experimental data were satisfied. Figure 12 is an example of comparing the turbulence models for prediction of the tangential velocity on the plane 160 mm from bottom of the tank. As can be seen, LES over-predicts the maximum of velocity, while RNG k-ε suffers from under-prediction. However, the maximum of tangential velocity on this plane is correctly captured with the DES turbulence model.

Other components of velocity and the turbulent kinetic energy predicted by the optimized model of each group on all planes were compared with the experimental data. The comparisons showed that the tangential velocity can be modelled with the renormalization group of k-ε turbulence model. Although the LES was successful for the computation of the radial and the axial velocity in some of the planes, its agreement with the experimental data did not show improvement over that achieved by RANS models such as RNG k-ε and transition SST. To predict the turbulent kinetic energy efficiently two of the RANS models, the three-equation model and the transition SST, had acceptable agreement. The Detached Eddy Simulation model, on the other hand, tended to under-predict the turbulent quantity which made it unsuitable candidate for the CFD problem of stirred tanks.

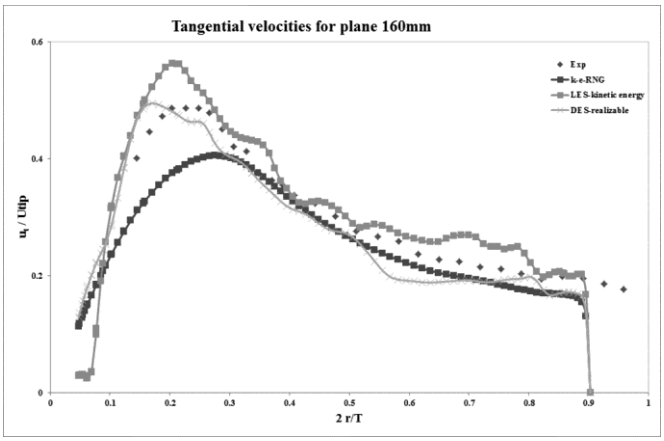

Fig. 12. Comparison of turbulence models with experimental data for tangential velocity on plane 160

5. Conclusion

Two underlying aspects of the numerical simulation of stirred tanks, namely the efficient grid scheme and the choice of suitable turbulence models, have been investigated. Through various criteria we have established the meshing methodology which ensures both results' independency and adequate agreement with experimental data. The widely used skewness factor was also tested to understand the optimal cell size in the bulk flow. The value of the y+ showed the problematic elements near the wall boundary conditions. Solving the problematic elements was carried out using different refinement methods to locally increase the number of cells. The grid independence study suggested that the solutions tend to converge at around 700,000 cells by which most characteristics of the turbulent flow can be captured.

In this study, the performances of RANS, LES and DES turbulence models for prediction of velocity components and turbulent kinetic energy have been investigated and compared with experimental data.

It was found that the RNG k-ε and the transition SST turbulence model produced better agreement for both velocity components and turbulent quantity. Likewise, the LES turbulence model in conjunction with the "kinetic energy" as subgrid-scale model was found to capture the trends of velocity components. However, the required CPU time for having converged solution made this model computationally intensive. Application of DES as the turbulence model for the stirred tank also gave accurate results for all the velocity components. It should be noted that the turbulent kinetic energy was under predicted.

Overall, this study demonstrated that for the consistent solution one needs to investigate the quality of mesh near the walls and the independency of the results from the number of cells. In addition, RANS turbulence models which implemented the Boussinesq hypothesis such as RNG k-ε and transition SST yielded better simulation of the flow behaviour inside the stirred tank. These recommendations might also be useful for the multiphase modelling of stirred tanks.

References

ANSYS Inc, 2009, *ANSYS FLUENT 12.0 Theory Guide*. ANSYS Inc,.

ARMENANTE, P.M., LUO, C., CHOU, C.-C., FORT, I., MEDEK, J., 1997, *Velocity profiles in a closed, unbaffled vessel: comparison between experimental LDV data and numerical CFD predictions*, Chemical Engineering Science 52(20), 3483–3492.

AUBIN, J., FLETCHER, D.F., XUEREB, C., 2004, *Modeling turbulent flow in stirred tanks with CFD: the influence of the modeling approach, turbulence model and numerical scheme*, Experimental Thermal and Fluid Science 28(5), 431–445.

BAKKER, A., OSHINOWO, L.M., 2004, *Modelling of Turbulence in Stirred Vessels Using Large Eddy Simulation*, Chemical Engineering Research and Design 82(9), 1169–1178.

BAKKER, A., OSHINOWO, L.M., MARSHALL, E., 2000, *The use of Large Eddy Simulation to study stirred vessel hydrodynamics*, In 10th European Conference on Mixing, 247–254.

CORONEO, M., MONTANTE, G., PAGLIANTI, A., MAGELLI, F., 2011, *CFD prediction of fluid flow and mixing in stirred tanks: numerical issues about RANS simulation*,Computer & Chemical Engineering 35(10), 1959–1968.

DEGLON, D.A., MEYER, C.J., 2006, *CFD modelling of stirred tanks: Numerical considerations*, Minerals Engineering 19(10), 1059–1068.

DONG, L., JOHANSEN, S.T., ENGH, T.A., 1994a, *Flow induced by an impeller in an unbaffled tank--I. Experimental*, Chemical Engineering Science 49(4), 549–560.

DONG, L., JOHANSEN, S.T., ENGH, T.A., 1994b, *Flow induced by an impeller in an unbaffled tank--II. Numerical modelling*, Chemical Engineering Science, 49(20), 3511–3518.

HINZE, J.O., 1975. *Turbulence*, Mc-Graw-Hill Publishing Co, New York.

KIM, W.-W., MENON, S., 1997, *Application of the localized dynamic subgrid-scale model to turbulent wall-bounded flows*, American Institute of Aeronautics and Astronautics.

LANE, G.L., SCHWARZ, M.P., EVANS, G.M., 2000, *Comparison of CFD methods for modelling of stirred tanks*, In 10th European Conference on Mixing, 273–280.

LAUNDER, B.E., SPALDING, D.B., 1972, *Lectures in Mathematical Models of Turbulence*, Academic Press, London, England.

MENTER, F.R., 1994, *Two-Equation Eddy-Viscosity Turbulence Models for Engineering Applications*, AIAA 32(8), 1598–1605.

MYERS, K.J., WARD, R.W., BAKKER, A., 1997, *A digital particle image velocimetry investigation of flow field instabilities of axial flow impellers*, Journal of Fluids Engineering 119, 623–632.

NICOUD, F., DUCROS, F., 1999, *Subgrid-Scale Stress Modelling Based on the Square of the Velocity Gradient Tensor*, Flow, Turbulence, and Combustion 62(3), 183–200.

ORSZAG, S.A., YAKHOT, V., FLANNERY, W.S., BOYSAN, F., CHOUDHURY, D., MARUZEWKI, J., PATEL, B., 1993, *Renormalization Group Modelling and Turbulence Simulations*, In International Conference on Near-Wall Turbulent Flows, Tempe, Arizona.

OSHINOWO, L., JAWORSKI, Z., DYSTER, K.N., MARSHALL, E., NIENOW, A.W., 2000. *Predicting the tangential velocity field in stirred tanks using the Mulkle Reference Frames (MRF) model with validation by LDV measurements*, In 10th European Conference on Mixing, 281-288.

SHIH, T.-H., LIOU, W.W., SHABBIR, A., YANG, Z., ZHU, J., 1995, *A new k-ε eddy viscosity model for high reynolds number turbulent flows*, Computers & Fluids 24(3), 227–238.

SHUR, M., SPALART, P., STRELETS, M., TRAVIN, A., 1999, *Detached-Eddy Simulation of an Airfoil at High Angle of Attack*, In 4th Int. Symposium on Eng. Turb. Modeling and Experiments, Corsica, France.

SMAGORINSKY, J., 1963, *General Circulation Experiments with Primitive Equations. I*, The Basic Experiment. Month. Wea. Rev 91, 99–164.

WILCOX, D.C., 1998, *Turbulence Modelling for CFD*, DCW Industries Inc., La Canada, California.

YOON, H.S., SHARP, K.V., HILL, D.F., ADRIAN, R.J., BALACHANDER, S., HA, M.Y., KAR, K., 2001. *Integrated experimental and computational approach to simulation of flow in a stirred tank*, Chemical Engineering Science 56(23), 6635–6649.